phys. stat. sol. (a) **138**, 89 (1993)

Subject classification: 61.70; 63.20; 78.30; S5

Bundesanstalt für Materialforschung und -prüfung, Berlin[1])

Diamonds for High Reflectivity (Normal Incidence) SR-Monochromators[2])

By

J. D. STEPHENSON

Theoretical (normal incidence) Bragg reflectivities from diamond are determined for several low/medium order reflections and found to be $\approx 10\%$ higher than those from Si or Ge. The angular positions of simultaneous (Renninger) reflections which reduce these intensities are also given and the possibilities of additional (secondary diffuse scattering) reflections are discussed. The calculations simulate the conditions expected from a diamond single crystal, used as a normal incidence SR-monochromator in a hard X-ray free electron laser (XFEL).

Die theoretische Bragg-Reflektivität (Senkrecht-Einstrahlung) von Diamant wird für Reflexe niedriger und mittlerer Ordnung berechnet und um etwa 10% über derjenigen von Si und Ge gefunden. Ebenso werden die Lagen der simultanen Renninger-Reflexe ermittelt, die die Intensität verringern. Das Auftreten zusätzlicher Reflexe (sekundäre diffuse Streuung) wird diskutiert. Die Berechnungen simulieren die Verhältnisse von Diamant-Einkristallen, die als Synchrotron-Monochromatoren hoher Reflektivität (senkrechter Einfall) für die hochauflösende Spektroskopie als fokussierende Synchrotron-Monochromatoren im Freien-Elektronen-(harten Röntgen-)Laser benutzt werden.

1. Introduction

In former papers, Stephenson [1, 2][3]) the excellent properties of type Ia diamonds (compared with type Ib and II diamonds, Si, Ge, and Be single crystals) were discussed concerning their use as *first* SR-monochromators in the present/future generation of high intensity (undulator/wiggler) beam lines. In particular, diamonds used as (back reflection) monochromators, have several important advantages relative to Si or Ge (Section 2). It is shown (Table 1) that Bragg %-reflectivities (R), calculated at nearly normal incidence for several major low/medium order reflections are superior ($\geqq 96.4\%$) to those from Si or Ge ($\leqq 88.7\%$). It is also well known that at exactly normal incidence the FWHM increases dramatically from *seconds* to *minutes* of arc (Kohra and Matsushita [3], Caticha and Caticha-Ellis [4]). Within such broad FWHM, the operative Bragg angle becomes relatively insensitive to small transient (thermal bump/mechanical) misalignments (an important condition for maintaining the stability of confocal/coincident X-ray free electron lasers (XFELs)). The angular positions of simultaneous Renninger reflections (which reduce the operative reflectivity, see Cole et al. [5]) are also given. Secondary diffuse scattering from diamond {100} planes containing nitrogen point defects (which strongly influence the {111}, {220}, and {113} reflections, Lonsdale and Smith [6]) are discussed.

---

[1]) Lab 6.22, Unter den Eichen 87, D-12203 Berlin 45, Federal Republic of Germany.

[2]) First presented in the DESY (Hamburg) Jahresbericht 1992 and ESRF (Grenoble), Oct. 1992.

[3]) In [2], p. 375, replace ^{14}C by ^{12}C.

The purpose of this report is to compare theoretical Bragg reflectivities at nearly normal incidence ($\theta_H = \pi/2 \pm 10^{-4}$ rad) for Ge, Si, and diamond and indicate the azimuthal angles at which Renninger reflections occur on rotation about the scattering vector (H).

2. Diamond SR-Monochromator

2.1 Advantages

Several important advantages exist when diamond is used as a Bragg SR-monochromator:

- sharper FWHM/higher energy resolution due to the smaller structure factors;
- higher Bragg reflectivities from reflections at normal incidence (this paper);
- minimised (diffracting surface) buckling/slope errors (due to their much higher thermal conductivity and lower thermal expansion coefficient (especially at 100 K, see Freund and Als-Nielsen [7];
- higher Debye temperature (i.e. $D_H \approx 1$ which allows higher-order reflections to be used).

The reduction in local buckling/slope errors (created on a monochromator surface by SR-heat loading) is currently judged by a 'figure of merit' which is the ratio of the coefficient of thermal conductivity (k) to the linear expansion coefficient (α). Values given in [7] give $(k/\alpha)_C = 33(k/\alpha)_{Si}$[4]), the higher the (k/α) value the lower the probability of local (heat-load) buckling causing wandering/instability in diffracted beam position. This is somewhat offset by the diamond lower specific heat which creates a relatively higher temperature increase in Si or Ge for the *same* incident SR-flux and which becomes more pronounced at low temperatures (100 K).

2.2 Normal incidence reflectivity calculations

In general, the approximations made in the standard presentation of the X-ray dynamical theory, neglect quantities smaller than the coefficient of electrical susceptibility ($\chi_H \approx 10^{-5}$ to 10^{-6}) which applies to Bragg angles $\theta_H \geq (\pi/2 \pm \Delta\theta)$ in which $\Delta\theta \approx 18.0$ mrad ($\approx 1°$ of arc). However, many well known relations (Zachariasen [8], Battermann and Cole [9]) fail if $\Delta\theta$ falls below this figure when not expanded from second- to fourth-order terms (Brümmer et al. [11], Fingerland [12], and [4]). Table 1 gives theoretical %-reflectivities for diamond obtained from these extended relations (see Appendix) using an incident Bragg angle of $\pi/2 \pm 10^{-4}$ rad ($\pm 20''$ of arc). Theoretically the FWHM of the C (diamond) 400-reflection at a Bragg angle of $\theta_{400} = 59.74°$ (operative wavelength $\lambda = 1.54052 \times 10^{-1}$ nm) is $\approx 2.76''$ which dramatically increases to $\approx 18'$ at the normal incidence position (operative wavelength $\lambda = 1.78349 \times 10^{-1}$ nm). SR-primary extinction coefficients ξ'_H (μm) are also given (see Appendix).

---

[4]) Figures of merit are dependent on k-values which are variable and (i) *statically* dependent on the type of diamond used (Burgemeister [10]) and (ii) *dynamically* dependent on the severity of the induced (interstitial) radiation damage.

Table 1
A comparison between diamond, Si, and Ge reflectivities (R) at $\theta_H = \pi/2 \pm 10^{-4}$ rad for $\tau = \pm 10^{-3}$*)

H	F'_H	F''_H	$\lambda(10^{-1}$ nm)	D_H	μ_0 (cm^{-1})	R (%)	$\Delta\theta_H$	ξ'_H (μm)
Ge	$a_0 = 5.657820 \times 10^{-1}$ nm		$\Delta a_0/a_0 = 8 \times 10^{-7}$		$\alpha = 5.6 \times 10^{-6}$ K^{-1}		$k = 0.7$ W × cm^{-1} K^{-1}	
220	179.3	(40)	4.00068	0.9660	5800	(66.6)	81.5′	2.1
400	151.4	(22.4)	2.82891	0.9330	2000	(76.4)	51.7′	3.7
422	133.9	13.84	2.30979	0.9010	1100	83.3	47.7′	4.3
440	118.6	11.20	2.00034	0.8710	750	80.9	31.2′	7.2
442	111.9	10.16	1.88594	0.8580	620	81.8	28.3′	8.2
620	110.0	9.44	1.78916	0.8480	515	83.4	26.5′	8.9
444	93.6	8.00	1.63327	0.8120	425	81.6	21.8′	11.9
642	82.8	6.40	1.45150	0.7920	300	83.5	18.8′	14.9
331	103.4	12.1	2.59598	0.9210	1500	70.2	38.9′	6.0
333/511	91.0	9.0	2.17769	0.8850	930	73.0	30.0′	8.4
Si	$a_0 = 5.430941 \times 10^{-1}$ nm		$\Delta a_0/a_0 = 2 \times 10^{-6}$		$\alpha = 2.3 \times 10^{-6}$ K^{-1}		$k = 1.6$ W × cm^{-1} K^{-1}	
220	69.3	11.20	3.84031	0.9698	2000	(69.0)	51.6′	5.0
400	59.6	7.70	2.71550	0.9406	750	78.6	33.2′	8.6
422	53.7	5.60	2.21720	0.9122	400	83.2	25.3′	12.0
440	48.4	3.80	1.920155	0.8847	270	84.2	20.5′	15.9
620	43.0	3.10	1.71744	0.8580	200	84.6	17.0′	20.6
444	39.9	2.64	1.56780	0.8321	146	86.1	14.7′	25.1
642	36.5	2.36	1.45150	0.8040	120	86.0	12.8′	30.7
311	45.4	6.71	3.27502	0.9450	1200	65.4	35.1′	9.3
331	41.0	4.70	2.49192	0.9290	560	73.9	25.1′	13.8
511/333	36.3	2.70	2.09040	0.9100	350	76.0	19.6′	18.9
531	33.8	2.40	1.83602	0.8700	230	79.5	16.2′	24.2
533	29.7	2.00	1.65644	0.8480	180	79.1	13.6′	31.3
711/551	27.2	1.80	1.52099	0.8250	135	80.7	11.8′	38.3
731/553	25.4	1.60	1.41411	0.7950	110	81.1	10.4′	45.8
dia-mond**)	$a_0 = 3.566986 \times 10^{-1}$ nm		$\Delta a_0/a_0 = 2.6 \times 10^{-6}$		$\alpha = 1.0 \times 10^{-6}$ K^{-1}		$k = 9.9$ to 26.2 W cm^{-1} K^{-1}	
220	15.29	0.208	2.52226	0.9983	72	97.1	30.1′	9.6
400	11.11	0.100	1.78349	0.9967	25	98.0	18.1′	18.8
422	10.50	0.065	1.45621	0.9950	12.5	98.7	14.4′	24.3
440	9.08	0.048	1.26113	0.9934	8.2	98.9	11.6′	32.6
442	8.70	0.042	1.18899	0.9926	6.9	98.9	10.7′	36.0
620	8.35	0.037	1.12798	0.9918	6.0	99.0	9.9′	39.7
444	7.20	0.030	1.02970	0.9901	4.8	99.0	8.4′	50.5
642	6.76	0.025	0.95332	0.9885	3.9	99.0	7.6′	58.1
311	9.00	0.105	2.15099	0.9977	45	96.3	19.7′	19.2
331	8.29	0.058	1.63664	0.9961	17	98.0	14.4′	27.4
511/333	7.21	0.039	1.37293	0.9944	10	98.4	11.3′	37.6
531	6.26	0.028	1.20586	0.9928	7.1	98.5	9.2′	49.4
533	5.70	0.020	1.08792	0.9911	5.5	98.6	7.9′	60.3
711/551	5.07	0.016	0.99895	0.9895	4.0	98.7	6.9′	73.9

*) a_0, α (see Hom et al. [13]) and k were measured at 298, 298, and 273 K, respectively.
**) Diamond F_H values are taken from Göttlicher and Wolfel [14], see also McConnell and Sanger [15].

3. Precautions

3.1 Renninger reflections

As the presence of multiple (Renninger) reflections ([5]) at normal incidence becomes increasingly critical, it is necessary to avoid them to retain the high operative reflectivities – an essential factor in achieving a positive energy gain factor in an XFEL. Table 2 compares

Table 2
Simultaneous reflections occuring at $\theta_H = \pi/2 - 10^{-4}$ rad, $H = (hkl)$ scattering vector (β can vary between $\pm 5°$ to $\pm 12°$ due to primary/secondary diffuse scattering)

H	refl. vector	λ (10^{-1} nm)	simult. refl.	β
even reflections				
220	$[1\bar{1}0]$	4.0006 (Ge)	(020, 200)	180.00°
		3.8403 (Si)	(020, 200)	360.00°
		2.5222 (C)		
400	[011]	2.8289 (Ge)	$(20\bar{2}, 202)$	35.26°
		2.7155 (Si)	$(2\bar{2}0, 220)$	144.73°
		1.7834 (C)	$(20\bar{2}, 202)$	215.26°
			$(2\bar{2}0, 220)$	324.73°
422	$[1\bar{1}\bar{1}]$	2.3097 (Ge)	(420, 402)	12.16°
		2.2172 (Si)	(400)	19.46°
		1.4562 (C)	(022)	160.53°
			(020, 002)	167.83°
			(402, 420)	192.17°
			(400)	199.48°
			(022)	340.52°
			(020, 002)	347.82°
442	$[1\bar{2}2]$	1.8859 (Ge)	(400)	4.93°
		1.8103 (Si)	(440)	15.79°
		1.1889 (C)	$(22\bar{2}, 224, 002)$	164.20°*)
			(040, 402, 042)	175.06°
			(400)	184.93°
			(440)	195.79°
			$(002, 224, 22\bar{2})$	344.20°*)
			(402, 042, 040)	355.06°
440	$[\bar{2}2\bar{2}]$	2.0003 (Ge)	(040, 400)	0.00°
		1.9201 (Si)	$(24\bar{2}, 42\bar{2}, 20\bar{2}, 02\bar{2},$	28.12°
		1.2611 (C)	202, 022, 242, 422)	
			(040, 400)	180.00°
			$(24\bar{2}, 42\bar{2}, 202, 022, 20\bar{2}, 02\bar{2},$	208.12°
			422, 242)	
444	$[1\bar{1}0]$	1.6332 (Ge)	(044, 440, 404, 040, 400, 004)	180.00°
		1.5678 (Si)	(044, 440, 404, 040, 400, 004)	360.00°
		1.0297 (C)		
620	$[1\bar{3}0]$	1.7891 (Ge)	$(4\bar{2}0, 2\bar{2}0, 240)$	21.41°
		1.7174 (Si)	(440, 020, 600)	158.58°
		1.1279 (C)	$(240, 2\bar{2}0, 4\bar{2}0)$	201.41°
			(020, 440, 600)	338.58°

Table 2 (continued)

H	refl. vector	λ (10^{-1} nm)	simult. refl.	β
642	[1$\bar{1}\bar{1}$]	1.5121 (Ge)	(602)	5.59°
		1.4515 (Si)	(640)	20.00°
		0.9533 (C)	(20$\bar{2}$, 444)	157.80°
			(40$\bar{2}$, 244)	158.40°
			(002)	160.00°
			(44$\bar{2}$, 600, 042, 204)	163.95°
			(24$\bar{2}$, 404)	169.73°
			(040)	174.40°
			(602)	185.60°
			(640)	200.02°
			(444, 20$\bar{2}$)	337.79°
			(244, 40$\bar{2}$)	338.40°
			(002)	339.97°
			(042, 204, 600, 44$\bar{2}$)	343.97°
			(404, 24$\bar{2}$)	349.73°
			(040)	354.40°
odd reflections				
553	[1$\bar{1}$0]	1.4730 (Ge)	(642, 462)	6.66°
		1.4141 (Si)	(620, 260)	7.51°
		0.9287 (C)	(42$\bar{2}$, 24$\bar{2}$, 315, 135)	168.63°
			(51$\bar{1}$, 15$\bar{1}$, 404, 044)	171.77°
			(3$\bar{1}$3, $\bar{1}$33, 1$\bar{1}$1, $\bar{1}$11)	173.34°
			(462, 642)	186.66°
			(620, 260)	187.52°
			(315, 135, 42$\bar{2}$, 24$\bar{2}$)	348.62°
			(404, 044, 51$\bar{1}$, 15$\bar{1}$)	351.77°
			(3$\bar{1}$3, $\bar{1}$33)	352.48°
			(1$\bar{1}$1, $\bar{1}$11)	353.34°
533	[01$\bar{1}$]	1.7256 (Ge)	(404, 440, 1$\bar{1}$3, 13$\bar{1}$)	176.22°
		1.6564 (Si)	(13$\bar{1}$, 1$\bar{1}$3, 440, 404)	353.34°
		1.0879 (C)		
531	[23$\bar{1}$]	1.9126 (Ge)	(440)	4.57°
		1.8360 (Si)	(333, 20$\bar{2}$)	151.43°
		1.2058 (C)	(42$\bar{2}$, 113)	152.83°
			(51$\bar{1}$, 022)	153.16°
			(3$\bar{1}\bar{1}$, 242)	157.39°
			(1$\bar{1}$1)	175.43°
			(440)	184.57°
			(20$\bar{2}$, 333)	331.44°
			(113, 42$\bar{2}$)	332.84°
			(022, 51$\bar{1}$)	333.16°
			(242, 3$\bar{1}$1)	337.39°
			(1$\bar{1}$0)	355.42°
331	[1$\bar{1}$0]	2.5959 (Ge)	(31$\bar{1}$, 13$\bar{1}$, 202, 022)	163.59°
		2.4919 (Si)	(202, 022, 31$\bar{1}$, 13$\bar{1}$)	343.59°
		1.6366 (C)		
311	[1$\bar{1}\bar{1}$]	3.4118 (Ge)	(1$\bar{1}$1)	7.22°
		3.2750 (Si)	(11$\bar{1}$, 220, 202)	172.78°
		2.1509 (C)	(1$\bar{1}$1)	187.22°
			(202, 220, 11$\bar{1}$)	352.78°

*) (222) negligible intensity.

the multiple reflections which occur at this orientation for several operative low/medium order reflections in Ge, Si, and C (diamond). Notice that the same multiple reflections occur at the same azimuthal angles (β) for each element which is a consequence of the (dia.) normal incidence condition where the RL-primitive translation(s), $b^* = \lambda/2a_0$ are constant. As an example, Fig. 1 shows a RL construction for the diamond (400), normal incidence reflection (operative wavelength 1.7834×10^{-1} nm). [011] is taken as the zero azimuthal position vector ($\beta = 0°$) from which the Ewald sphere is rotated about the $\boldsymbol{H}_{400}$ scattering vector. At $\beta = 35.26°$ and 215.26° the (202) and (20$\bar{2}$) RL points (Renninger reflections) move into the sphere. The diagram also shows presumed primary and secondary diffuse scattering regions around given RL points (left side inset) which in an extreme case extends the Bragg reflection range by $\pm 5°$ (primary) and/or $\pm 12°$ (secondary). In this context the imaginary shapes of the {111}, {220}, and {113} RL points (presumed from the experiments in [6]) are displayed in three modes: (i) a dark central spherical spot implying the (isotropic) thermal Debye-Waller vibration associated with each plane (which remains a relative constant for most diamond reflections due to the high Debye temperature factor), (ii) an outer (fainter) region of *isotropic* primary mosaic diffuse scattering (which is present in type II and Ib diamonds but not in a relatively perfect type Ia diamond), and (iii) six-fold ⟨100⟩ spike regions representing (inherent static nitrogen point defect) secondary diffuse scattering (which is present in type I but not in type II diamonds).

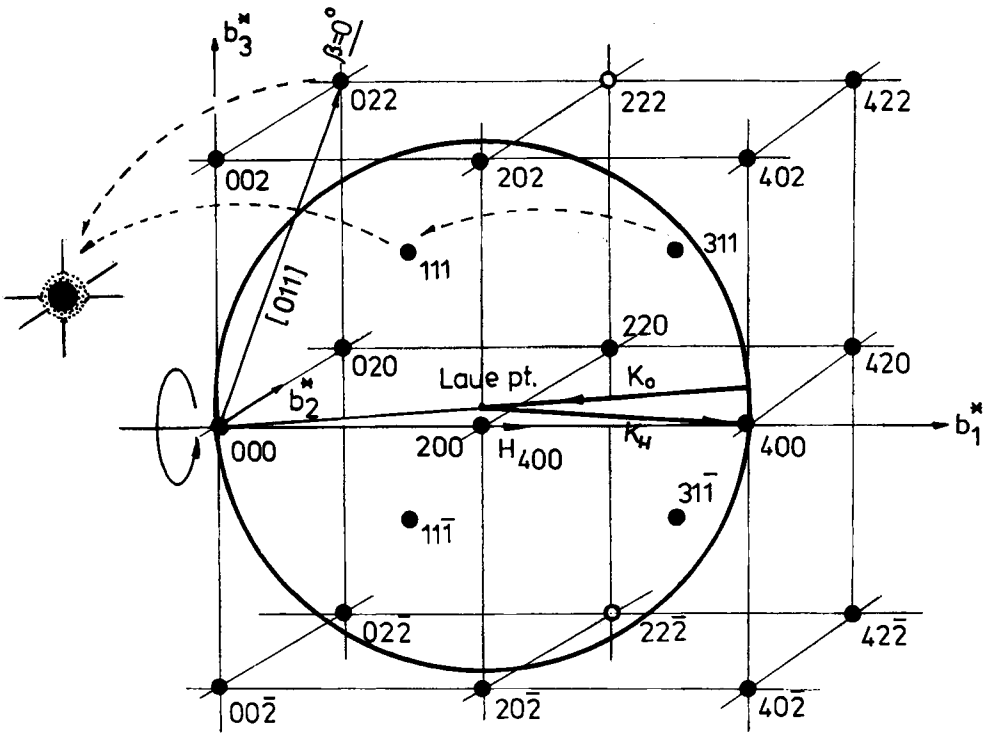

Fig. 1. Diamond (400)-RL at nearly normal incidence showing {202} multiple reflections which enter the Ewald sphere at $\beta \approx 35°$ and 215° and the presumed shapes of the RL (diffuse scattering) points (left inset)

3.2 Energy/wavelength resolution

In general the diamond energy/wavelength resolution is critically dependent on changes in (i) temperature (expansion/contraction), (ii) dilation (point defect density/applied strain/bending), and (iii) radiation damage (interstitial production).

These are included in the well-known energy/wavelength resolution equation as

$$|\Delta E/E| = \Delta\lambda/\lambda = \cot\theta_H \, \Delta\theta_H + \sum_{i=1}^{n} (\Delta d_H/d_H)_i \,, \tag{1}$$

which at nearly normal incidence approximates to

$$|\Delta E/E| = \Delta\lambda/\lambda = (\delta\theta_0 - \tau)\, \Delta\theta_H + \sum_{i=1}^{n} (\Delta d_H/d_H)_i \qquad (\delta\theta_0 - \tau \leqq 10^{-3}) \,, \tag{2}$$

in which i refers to the number of different ways in which lattice dilation/strain can be introduced, e.g. by

– local thermal bump gradients, generated at the monochromator surface which are minimized using high thermal conductivity diamond, cooled to 100 K [7]. The thermal strain is given by

$$(\Delta d_H/d_H)_T = \alpha_C \, \Delta T \,, \tag{3}$$

where α_C ($\approx 2.6 \times 10^{-6}$) is the coefficient of linear expansion and ΔT the temperature gradient normal to the surface;

– bending (e.g., by focussing or by cooling water pressure on the rear side (Berman et al. [16])). Three-point bending creates a strain, normal to the surface (Moncton [17]) given by

$$\Delta\varepsilon_z = (\Delta d_H/d_H)_z = -2\mu \, \Delta z/R(1 - \mu) \,, \tag{4}$$

where μ is Poisson's ratio and R the radius of curvature. Experimentally $\mu_{Si} = 0.3$ whilst for diamond, μ_C varies between 0.1 and 0.29 ($\bar{\mu}_C = 0.2$, Howes [18]) giving strains, $\Delta\bar{\varepsilon}_C = -2.5 \times 10^{-5}$ and $\Delta\varepsilon_{Si} = -4.5 \times 10^{-5}$ throughout a depth $\Delta z = 100\,\mu$m with $R = 2$ m. (The standard remedy of cutting fingers (1 mm^2, 0.8 mm deep) into the surface, to eliminate this effect, is not a complete solution since this increases the point defect concentration at the cut edges and deteriorates the crystal (pendellösung) perfection, Stephenson [19]);

– high energy X-, γ-ray photon radiation damage by which (mainly interstitial) bulk dilation is created and which increases with exposure time.

In all cases the value of $\Delta E/E$ depends on whether the total dilation sum is greater or less than $(\delta\theta_0 - \tau)\, \Delta\theta_H$ and as a concluding remark it should be noted that at nearly normal incidence $\Delta\theta_H$ ($\approx$ FWHM) increases by two orders of magnitude (see Table 1) which can result in values ($\geqq 10^{-6}$) for the first term on the right of (1). Without bending this gives a resultant $|\Delta E/E| \geqq 10^{-6}$ which will eventually increase with high X- and γ-ray irradiation damage; with bending it will increase to $\geqq 10^{-5}$.

Appendix

Expanded (complex) quantities, used in the (normal incidence) reflectivity calculations

Using the expansions in [4], with reference to Fig. 2 and [9], the (directly) measurable Bragg reflection coefficient, R (or power ratio), for a centrosymmetric crystal is

$$R = |D_H/D_0|^2 = |b| \, \{L - \sqrt{(L^2 - 1 - 4x^2)}\} \; (\sigma\text{-polarization}) \,, \tag{5}$$

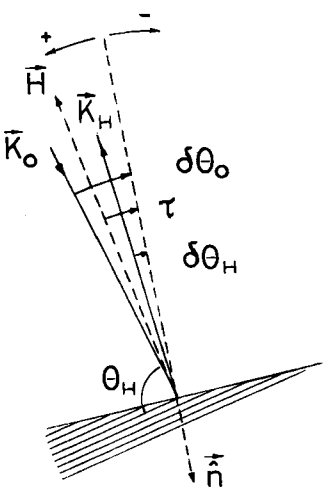

Fig. 2. Parameters used at normal incidence

where

– D_0 and D_H are the incident and diffracted electric displacement amplitudes;

– $b = \chi_0 - 2\tau\,\delta\theta_0 - 1$;

– $\tau = \tan(\hat{\boldsymbol{n}} \cdot \hat{\boldsymbol{H}})$, $\hat{\boldsymbol{n}} \cdot \hat{\boldsymbol{K}}_0 = \delta\theta_0$, $\hat{\boldsymbol{n}} \cdot \hat{\boldsymbol{K}}_H = \delta\theta_H$ (where $\hat{\boldsymbol{n}}$ is the inward unit vector surface normal, $\hat{\boldsymbol{K}}_0$, $\hat{\boldsymbol{K}}_H$ and $\hat{\boldsymbol{H}}$, the unit vectors of the incident, diffracted, and scattering waves, respectively;

– (corrected values, $\delta\theta_0 = -\delta\theta_H - \tau\,\delta\theta_H^2/2 - 2\tau\varepsilon$ with $\varepsilon = (\chi_0' - \delta\theta_0^2)/2$ were used);

– $\varkappa = \chi_H''/\chi_H'$ in which $\chi_H = -r_0\lambda^2 F_H D_H/\pi\Omega$ is the Fourier component of the electric susceptibility for reflection $H = hkl$, λ the operative wavelength, r_0 the classical electron radius, and Ω the unit cell volume. F_H is the unit cell structure factor and D_H the (isotropic) Debye-Waller factor;

– $\Delta\theta_H$ ($\approx$FWHM) $= 2\sqrt{|\chi_H|}$ at the normal incidence position;

– $\theta_H = \pi/2 \pm 10^{-4}$ rad is the (normal incidence) Bragg angle range used in the calculations;

– $\chi_0'' = -\mu_0\lambda/2\pi$ where μ_0 is the average linear absorption coefficient;

– diamond (isotropic) Debye-Waller factors were determined using an atomic mean square vibrational amplitude of $\bar{u}_C^2 = 0.004 \times 10^{-2}$ nm^2 (Lonsdale [20]);

– the angular position of the diffracted beam profile (including absorption) is represented by the complex parameter

$$y = \{\chi_0(1 - b) + ab\}/2\sqrt{|b|}\,|\chi_H| \quad \text{(centrosymmetric)}, \tag{6}$$

where $\alpha = \chi_0(2 - \delta\theta_0^2)$, which determines

$$L = |y^2| + |g^2| + |\sqrt{(y^2 - g^2 - 1)^2 + 4(gy - \varkappa)^2}| \quad \text{(thick crystal)}, \tag{7}$$

in which $g = (1 - b)\,\chi_0''/(2\,|\chi_H'|\sqrt{|b|})$.

SR-primary extinction coefficients (1/100 attenuation of the beam, see [14]) are given by

$$\xi_H' = 4.61\Omega/2r_0\lambda\,|F_H|\,. \tag{8}$$

References

[1] J. D. STEPHENSON, Hasylab Jahresbericht, 1987 (p. 208).
[2] J. D. STEPHENSON, phys. stat. sol. (a) **134**, 374 (1992).
[3] K. KOHRA and T. MATSUSHITA, Z. Naturf. **27a**, 484 (1972).
[4] A. CATICHA and S. CATICHA-ELLIS, Phys. Rev. B **25**, 97 (1982).
[5] H. COLE, F. W. CHAMBERS, and H. M. DUNN, Acta cryst. **15**, 138 (1962).
[6] K. LONSDALE and H. SMITH, Nature **148**, 112, 257 (1941).
[7] A. K. FREUND and J. ALS-NIELSEN, ESRF News Report, April 1992.
[8] W. H. ZACHARIASEN, Theory of X-Ray Diffraction in Crystals, Dover, New York 1967.
[9] B. W. BATTERMAN and H. COLE, Rev. mod. Phys. **36**, 681 (1964).
[10] E. A. BURGERMEISTER, Physica (Utrecht) **B93**, 165 (1978).
[11] O. BRÜMMER, H. R. HÖCHE, and J. NIEBER, phys. stat. sol. (a) **53**, 565 (1979).
[12] A. FINGERLAND, Acta cryst. **A27**, 280 (1971).
[13] T. HOM, B. KISENICK, and B. POST, J. appl. Cryst. **8**, 457 (1975).
[14] S. GÖTTLICHER and W. WOLFEL, Z. Electrochem. **63**, 891 (1959).
[15] J. F. MCCONNELL and P. L. SANGER, Acta cryst. **A26**, 83 (1970).
[16] L. BERMAN, M. HART, and S. SHARMA, Nuclear Instrum. and Methods A **321**, 617 (1992).
[17] D. MONCTON, Collected Papers, Summer School on X-Ray Scattering with SR, Vienna, Sept. 1980, Technische Hochschule Wien.
[18] V. R. HOWES, Physical Properties of Diamond, Ed. R. BERMAN, Clarendon Press, Oxford 1965 (p. 174).
[19] J. D. STEPHENSON, phys. stat. sol. (a) **115**, 97 (1989).
[20] K. LONSDALE, Acta cryst. **1**, 142 (1945).

(Received March 2, 1993; in revised form April 28, 1993)